Magnesium Boride Nanotubes: Relative Stability and Atomic and Electronic Structure

Pavel B. Sorokin,*,†,‡,∥ Leonid A. Chernozatonskii,∥ Pavel V. Avramov,†,§ and Boris I. Yakobson‡

Siberian Federal University, 79 Svobodny Avenue, Krasnoyarsk, 660041 Russian Federation, Department of Mechanical Engineering & Material Science and Department of Chemistry, Rice University, Houston, Texas 77251, Emanuel Institute of Biochemical Physics, Russian Academy of Sciences, 4 Kosigina Street, Moscow, 119334, Russian Federation, and Kirensky Institute of Physics, Russian Academy of Sciences, Akademgorodok, Krasnoyarsk, 660036 Russian Federation

Received: November 25, 2009; Revised Manuscript Received: February 5, 2010

A comparative study of the energies and the electronic structure of MgB_x nanotubes is performed within the framework of the density functional theory. Different basic compositions ($x = 2$ for diboride and $x = 3$ for triboride) and different diameters (3 Å $< D <$ 18 Å), as well the exterior, interior, and staggered placement of magnesium atoms, are considered. Energy analysis reveals a nontrivial bending behavior of the MgB_2 sheets, such that the tubes with exterior and staggered configurations display the energy minima at certain small diameters (of the boron cage sublattice). The semiconducting behavior of narrow MgB_2 nanotubes with exterior Mg position was observed.

1. Introduction

Magnesium diboride based materials have attracted a lot of attention because of their remarkable physical properties and wide possible technological applications. Special interest in the crystalline MgB_2 has ignited after discovery of the magnesium diboride superconductivity at 39 K.[1] The MgB_2 nanotubes are expected to display the same remarkable physical properties caused by layered atomic structure of the parent material, bulk magnesium diboride.

Using simple classical analysis, the existence of MgB_2 nanotubes of two isomorphic configurations has been suggested, with interior and exterior magnesium layers relative to the boron lattice. The energies of armchair and zigzag tubes were approximately evaluated,[2] showing that the armchair nanotubes of the first configuration with interior magnesium layer are energetically preferable. On the other hand, the paper by Lau et al.[3] reported a single narrow zigzag MgB_2 nanotube, while focusing on different concentrations of magnesium atoms (all exterior) on a boron cage, concluding that the Mg tends to distribute uniformly.

Further, the electronic structure of selected four armchair MgB_2 nanotubes of both configurations[4] was studied using the density functional tight binding (DFTB) method. The DFTB approach confirmed the energetic stability of the first configuration with interior magnesium layer. Another study[5] reported DFT calculations of a MgB_2 nanotube with the exterior (with respect to the boron cage) magnesium layer. The crystalline tubular structure based on the MgB_2 nanotubes has also been studied using DFT calculations.[3,6] Overall, it was shown that all MgB_2 nanotubes and related structures display metallic properties.[3–6]

In another line of recent research of the most favorable boron atom arrangement in the pure-boron hollow clusters (boron fullerenes[7–11] and nanotubes[12–14]), the original Aufbau principle for boron clusters[15,16] was modified.[7] It was found that the periodic exclusion of boron atoms from the uniform triangular boron lattice of hollow clusters leads to improved energetic stability.[17] In the case of curved clusters, the effect can be additionally interpreted in the following way. The curvature of a cluster increases the tension of the atomic structure, and an insertion of empty hexagons (or removal of some boron atoms) decreases it. Along with this, on the other hand, the deletion of selected boron atoms deviates from the Aufbau principle and thus decreases the stability of the structure. The "golden mean" in the competition of both effects is the 1/3 ratio between the number of empty and filled boron hexagons/pentagons in the atomic geometry of the boron clusters.[7] One can similarly suggest that the modified Aufbau principle[7] can also be applied to other boron-based nanoclusters, e.g., in transforming MgB_2 into MgB_3 nanotubes.

Motivated initially by this possibility of varying the composition and structure−property relationship of MgB_x ($x > 0$) nanotubes, we systematically designed and studied the atomic makeup and electronic properties of MgB_2 and MgB_3 compositions in different isomorphic configurations. It becomes of particular interest due to the recent report of microscopy observations of the large diameter MgB_2 nanotubes and their superconductivity.[18] The experimental observations of other metal boride (Fe−B, Co−B, and Ni−B) nanotubes[19] further support the feasibility of the MgB_x family as well.

2. Method and Model

The calculations of the atomic and electronic structure of magnesium diboride and tridoride nanotubes (MgB_2-NT and MgB_3-NT) were performed using density functional theory[20,21] within the local density approximation for the exchange-correlation functional,[22] employing norm-conserving Troullier−Martins pseudopotentials[23] in the Kleinman−Bylander factorized form.[24] Finite-range numerical pseudoatomic wave functions

* Corresponding author. E-mail: PSorokin@iph.krasn.ru.
† Siberian Federal University.
‡ Rice University.
∥ Emanuel Institute of Biochemical Physics, Russian Academy of Sciences.
§ Kirensky Institute of Physics, Russian Academy of Sciences.

10.1021/jp9112014
Published on Web 03/02/2010

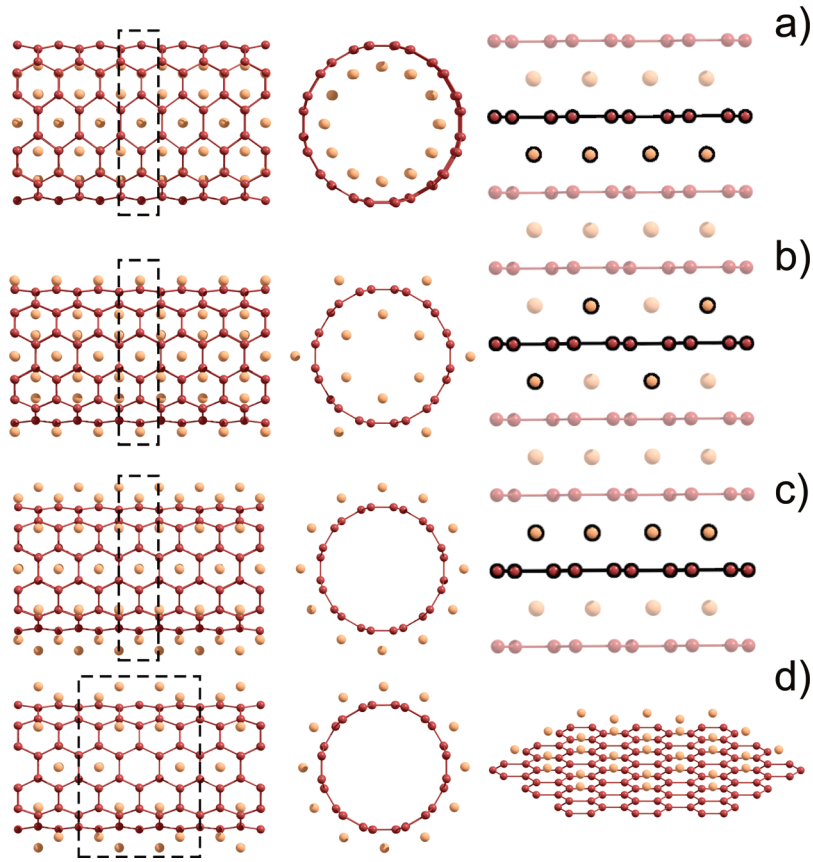

Figure 1. Atomic structure of (6, 6) MgB_2 armchair nanotubes with interior (a), staggered (b), and exterior (c) Mg layers. MgB_2 crystalline lattice, with highlighted atoms isomorphic to the corresponding nanotubes, is presented on the right-hand side of the figure. (d) Structure of {6, 0} MgB_3 nanotube and the perspective view of a MgB_3 single layer. The unit cells of the tubes are marked by dotted rectangles.

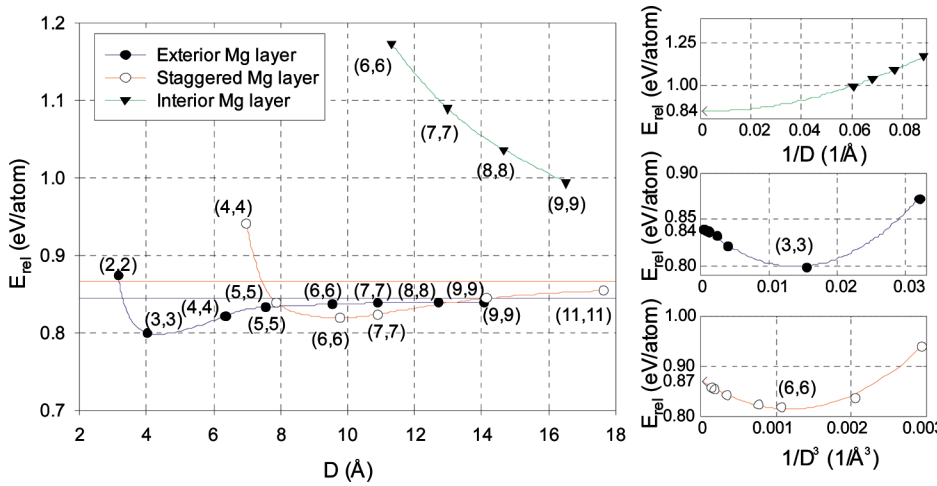

Figure 2. Dependence of the relative (E_{rel}) energy of magnesium diboride nanotubes upon the diameter (D) of corresponding boron cages. The energy dependence of the tubes with interior Mg configuration is presented as a green line with solid triangles. The energy dependence of the tubes with staggered Mg configuration is presented as a red line with empty circles. The energy dependence of the tubes with exterior Mg configuration is presented as a blue line with solid circles. The energies of a single MgB_2 layer with exterior and staggered magnesium layer is presented as blue and red horizontal solid lines, respectively. In the insets the dependences of relative energies of magnesium diboride nanotubes upon inverse diameter (MgB_2-NT with interior magnesium layer) and inverse diameter in the third power (MgB_2-NT with exterior and staggered magnesium layer) are shown.

were used as an atomic orbital basis set. Nanotubes were treated in a tetragonal supercell scheme allowing enough empty space between them to make intermolecular interactions negligible. The geometry of the structures was optimized until residual forces became less than 0.04 eV/Å. The real-space mesh cutoff was set higher than 125 Ry. The Monkhorst−Pack[25] special k-point scheme was used with 0.1 $Å^{-1}$ k-point spacing. We used the SIESTA package[26,27] in all calculations. All the values given above were carefully tested and found optimal.

3. Results and Discussion

3.1. Atomic Structure. The MgB_2 nanotubes consist of several concentric cylinders formed by rolled hexagonal magnesium and boron graphite-like plane networks. Alternatively,

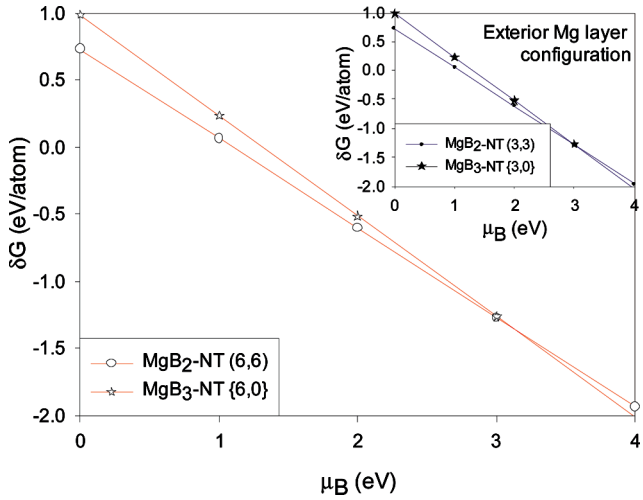

Figure 3. Gibbs free energies of formation of the (6, 6) MgB_2-NT (red line with empty circles) and {6, 0} MgB_3-NT (red line with empty stars) with staggered magnesium layer configuration, plotted as a function of the boron chemical potential μ_B (shifted to the value of μ_B in the $R\bar{3}m$ solid state boron phase). In the inset the similar dependencies of Gibbs free energies of formation of (3, 3) MgB_2-NT (blue line with filled circles) and {3, 0} MgB_3-NT (blue line with filled stars) with exterior magnesium layer configuration are presented.

one can view the atomic structure of MgB_2 nanotubes as a boron hexagonal framework with magnesium atoms in the centers of the hexagons.[2] First predictions of the metal boride nanotubes with such structure have been made concurrently by Quandt et al.[28] (for AlB_2) and Chernozatonskii[2] (for MgB_2).

We studied three different configurations of magnesium ion arrangement relative to the boron framework: interior (with interior magnesium layer, Figure 1a), intermediate staggered (with interior and exterior magnesium layers, Figure 1b), and exterior (with exterior magnesium layer, Figure 1c) configurations. To clarify the structure of the tubes, we also present (on the right of Figure 1) the atomic lattice of the bulk MgB_2 and highlight the atoms involved in the corresponding nanotube constructions. We investigated only armchair tubes because our preliminary calculations and the data from refs 2 and 4 give evidence that these are most energetically favorable structures.

To introduce classification of MgB_3 nanotubes, let us follow the classification of boron tubes.[12–14] It is necessary to note that the basis vectors of the precursor boron plane are turned 30° relative to the corresponding hexagonal graphene lattice. Following classification[12–14] the MgB_3 nanotubes $\{N, M\}$ can be divided into three classes: (i) zigzag nanotubes with $N = M$, (ii) armchair nanotubes with $N \neq 0$ and $M = 0$, and (iii) chiral nanotubes with $N \neq M$. As an example the atomic structure of {6, 0} MgB_3 armchair nanotube is presented in Figure 1d.

Strictly speaking, the MgB_2 nanotubes with staggered magnesium layer have different classification from MgB_2-NT with exterior and interior magnesium layer because of the twice bigger lattice vectors of the basis layer of the tubes. But for comparison we use the common classification for all MgB_2-NT.

3.2. Energetic Properties. To evaluate relative stability, it is convenient to compare the energy of a MgB_2 nanotube (Figure 2) with the energy of bulk MgB_2 material, per atom (essentially, the formation energy of a tube from bulk crystal)

$$E_{rel} = E^{tube} - E^{bulk}$$

where E^{tube} refers to the tube and E^{bulk} is the energy of bulk magnesium diboride. Choosing the energies per atom rather than per formula unit has an advantage when one wants to compare different compositions, such as MgB_2 and MgB_3 in the present case.

With increasing diameter D, the energies of MgB_2 tubes with exterior and staggered magnesium layers approach the energy of planar MgB_2 sheet, and each has a minimum at a certain D of the boron cages, in contrast to the carbon single-wall nanotubes, for which $E(D) \sim 1/D^2$ is monotonous.[29] The energy dependence can be formally approximated by the $E(D) = A((1/D^3) - (1/D_0^3))^2 - B$. In the case of MgB_2-NT with exterior magnesium layer, $A = 230$ (eV·Å^6/atom) and $B = 0.80$ eV/atom. The minimum D_0 of the curve corresponds to the favorable structure and is equal to 4.2 Å, which is close to the diameter of the (3, 3) tube (4.0 Å). For MgB_2-NT with staggered magnesium layer, $A = 41 \cdot 10^3$ (eV·Å^6/atom) and $B = 0.81$ eV/atom with D_0 equal to 9.4 Å, which is close to the 9.8 Å diameter of the (6, 6) tube. (The accuracy of the fitted coefficients is based on adjusted $R^2 > 0.98$ in all cases.)

The energy dependences of the tubes tend to the energies of corresponding MgB_2 sheets ($E(\infty)$ of MgB_2-NT with exterior configuration is equal to 0.84 eV/atom; $E(\infty)$ of MgB_2-NT with staggered configuration is a little bit larger and is equal to 0.87 eV/atom). The nonmonotonic energy dependence behavior was also found for SiO_2,[30,31] C_2F,[32] and SiH[33] nanotubes. The energies of (n, n) tubes with exterior magnesium layers for $n > 9$ are lower than the corresponding energies of the tubes with staggered magnesium layers. This result means that MgB_2 tubes with diameters $D < 8$ Å and $D > 14$ Å more likely contain magnesium layer with exterior configuration, whereas tubes with diameters 8 Å $< D <$ 14 Å would rather contain magnesium layer with staggered configuration.

The planar MgB_2 sheet is less stable than most tubes with exterior and staggered magnesium layers. Such low stability of single MgB_2 sheet was predicted by Chernozatonskii[2] and Saito et al.[5] The atomic sheets in graphite are bounded by weak van der Waals forces and can be roughly treated as independent, whereas the ionic interlayer interaction in bulk MgB_2 is much stronger.[5] Therefore, it is possible to obtain the single layer of graphite,[34] whereas obtaining a single flat layer of MgB_2 seems to be unrealistic.

Mg−Mg interactions in the tubes make the main contribution to the stability of the staggered configuration. Distances between neighboring magnesium ions in both interior and exterior layers in the favorable MgB_2 (6, 6)-NT are close to the bulk value of 3 Å,[1] whereas for tubes with other diameters this value is noticeably different. The most energetically favorable tubes with exterior Mg layer display Mg−B distances closest to the bulk values.

The dependence of the relative energy on diameter D of MgB_2-NT with interior Mg configuration displays monotonic behavior due to repulsion of interior magnesium ions. Because of this, the (n, n) tubes with $n < 6$ are unstable. The best fit of the energy dependence is inversely quadratic $E(D) = A(1/D)^2 + E_0$, where $A = 41.64$ (eV·Å^2/atom) and $E_0 = 0.843$ (eV/atom) is the strain energy of the single MgB_2 sheet. The interior magnesium ions visibly expand the boron cage, and therefore diameters of the tubes are much bigger than the diameters of corresponding tubes with exterior and staggered Mg configurations. Our results are different from the DFTB results of Ivanovskaya et al.[4] who reported that nanotubes with interior magnesium layer are energetically more favorable.

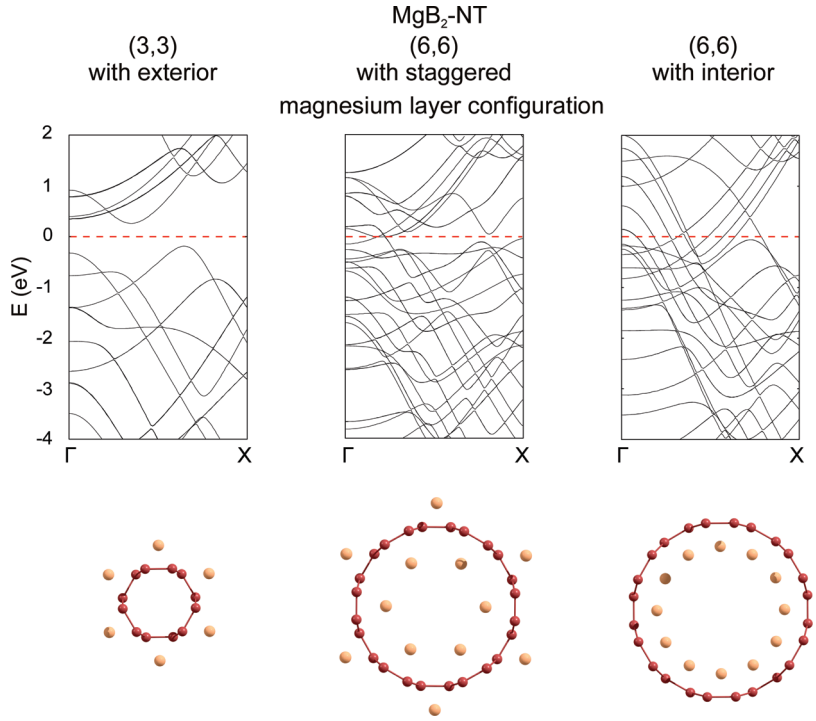

Figure 4. Electronic band structure of MgB_2 nanotubes. (3, 3) MgB_2 with exterior, (6, 6) staggered, and (6, 6) interior Mg layer configurations and corresponding nanotube cross sections. The Fermi level is shifted to zero and marked by the dotted horizontal line.

The relative stability of MgB_x-NT of different stoicheometry x depends of course on the constituents' chemical potentials, μ_{Mg} for magnesium and μ_B for boron, which in turn represent environmental conditions of synthesis. To account for this effect, we used the Gibbs free formation energy δG[35] for the MgB_x, as

$$\delta G(x, \mu_B) = E^{\text{total}}(x) - \mu_{Mg} - x\mu_B$$

The dependence of $\delta G(x, \mu_B)$ on μ_B for MgB_x-NT systems is depicted in Figure 3. When choosing the μ_{Mg} and μ_B, we do not try to suggest specific synthetic conditions (generally a daunting task for theory), but simply select some realistic values for the constituent elements and evaluate the (meta)stability of MgB_x tubes with respect to possible decomposition/segregation into pure B and pure Mg. To compare the relative stability of MgB_x-NT for different x, the value μ_{Mg} was fixed and equal to the chemical potential of bulk magnesium (P 63/mmc). The value μ_B was chosen to vary due to the existence of a set of boron allotropes in nature. One can imagine a possible situation when MgB_x is obtained by reacting a B-containing vapor component with Mg substrate, in a CVD-type approach. In this case μ_B varies by experimental conditions (pressure, temperature, and B-feedstock choice).

The μ_B parameter can be calculated by the same method for $R\bar{3}m$[36] ($\mu_B^{R\bar{3}m}$) and $P\bar{4}n2$[37] ($\mu_B^{P\bar{4}n2}$) symmetries of two different phases of boron.In the case of the $\mu_B^{R\bar{3}m}$, the (6, 6) MgB_2-NT is ~0.26 eV/atom more thermodynamically stable than the {6, 0} MgB_3-NT. Another μ_B value for the $P\bar{4}n2$ ($\mu_B^{P\bar{4}n2} - \mu_B^{R\bar{3}m} = 0.12$ eV/atom) leads to decreasing of the difference between the (6, 6) MgB_2-NT and {6, 0} MgB_3-NT energies up to ~0.25 eV/atom. The MgB_3 phase can become more favorable only at $\mu_B > 3.06$ eV (Figure 3).

3.3. Electronic Structure. Similar to crystalline MgB_2, all examined MgB_2 nanotubes, except the (2, 2) ($E_{gap} = 0.63$ eV) and (3, 3) ($E_{gap} = 0.45$ eV, Figure 4a) MgB_2-NT with exterior Mg arrangement, display metallic properties. Increase of the MgB_2 nanotube diameter leads to the closing of the band gap and restoring the metallic behavior. The presence of the nonzero band gap in MgB_2 tubes with diameters $D < 5$ Å can be attributed to the strain in the atomic structure caused by large nanotube curvature.

4. Conclusions

A comparative study of MgB_x nanotubes extends the previous knowledge[2–6] and reveals the preferred composition, sublattices (Mg versus B) spatial organization, and diameters. Novel MgB_2 nanotubes with staggered magnesium layer configuration are predicted as a possibility, and the energy change caused by curvature strain is related to the nanotube diameter. It is found that the energy curves of the energetically favorable MgB_2 tubes with exterior and staggered magnesium layer configurations have a pronounced minimum at some preferred diameters of the boron cage. The energy curves of the less favorable MgB_2 tubes with interior magnesium layer are monotonous and rather high. The energy dependencies of all tubes tend to the energy of the corresponding planar MgB_2 sheets. MgB_2 tubes with exterior magnesium layer with diameters smaller than 8 Å and bigger than 14 Å are energetically favorable, whereas tubes with staggered magnesium layer are favorable with diameters between 8 and 14 Å. It was found that MgB_2-NT are generally energetically preferable over the MgB_3 tubes. All examined MgB_2 nanotubes display metallic properties except very narrow diameter tubes. The proposed MgB_2 nanotubes can be (if their synthesis[18] is further refined) used in nanoelectronics as interconnects. Observation of superconductivity in magnesium diboride nanotubes[18] opens even more tantalizing possibilities for such one-dimensional structures. Further, recent prediction of high hydrogen adsorption on TiB_2 nanotubes[38] suggests a similar property possibly for MgB_2 structures as well.

Note Added in Proof. After completion of the present study, we became aware of comprehensive comparison[39] of various

geometries of MgB_2 layer, which can also be rolled into stable MgB_2 nanotubes. This elegant approach can also be applied to test other stoichiometries Mg_xB_{1-x}, however comparison across the different compositions will depend on the choice of elemental chemical potentials.

Acknowledgment. P.B.S. and B.I.Y. acknowledge support by the Basic Energy Sciences division of the Department of Energy, award DE-SC0001479. L.A.C. was supported by the Russian Academy of Sciences, program No. 21. P.V.A. and P.B.S. also acknowledge the collaborative RFBR-JSPS grant No. 09-02-92107-ЯФ. We are grateful to the Joint Supercomputer Center of the Russian Academy of Sciences for the possibility of using a cluster computer for quantum chemical calculations. The geometry of all presented structures was visualized by commercial ChemCraft software (http://www.chemcraftprog.com).

References and Notes

(1) Nagamatsu, K. J.; Nakagawa, N.; Muranaka, T.; Zenitani, Y.; Akimitsu, J. *Nature* **2001**, *410*, 63.
(2) Chernozatonskii, L. A. *JETP Lett.* **2001**, *74*, 335.
(3) Lau, K. C.; Orlando, R.; Pandey, R. *J. Phys.: Condens. Matter* **2009**, *21*, 045304.
(4) Ivanovskaya, V. V.; Enjashin, A. N.; Sofronov, A. A.; Makurin, Yu.N.; Medvedeva, N. I.; Ivanovskii, A. L. *J. Mol. Struct.* **2003**, *625*, 9.
(5) Saito, S.; Louie, S. G.; Cohen, M. L. *J. Phys. Soc. Jpn.* **2007**, *76*, 043707.
(6) Prasad, D. L. V. K.; Jemmis, E. D. *J. Mol. Struct.: THEOCHEM* **2006**, *771*, 111.
(7) Szwacki, N. G.; Sadrzadeh, A.; Yakobson, B. I. *Phys. Rev. Lett.* **2007**, *98*, 166804.
(8) Zope, R. R.; Baruah, T,; Lau, K. C.; Liu, A. Y.; Pederson, M. R.; Dunlap, B. I. *Phys. Rev. B* **2009**, *79*, 161403.
(9) Sadrzadeh, A.; Pupysheva, O. V.; Singh, A. K.; Yakobson, B. I. *J. Phys. Chem. A* **2008**, *112*, 13679.
(10) Mukhopadhyay, S.; He, H.; Pandey, R.; Khin, Y.; Boustani, I. *J. Phys.: Conf. Ser.* **2009**, *176*, 012028.
(11) Li, M.; Li, Y.; Zhou, Z.; Shen, P.; Chen, Z. *Nano Lett.* **2009**, *9*, 1944.
(12) Yang, X.; Ding, Y.; Ni, J. *Phys. Rev. B* **2008**, *77*, 041402.
(13) Singh, A. K.; Sadrzadeh, A.; Yakobson, B. I. *Nano Lett.* **2008**, *8*, 1314.
(14) Chernozatonskii, L. A.; Sorokin, P. B.; Yakobson, B. I. *JETP Lett.* **2008**, *87*, 489.
(15) The Aufbau principle says that highly stable boron nanoclusters, surfaces, and networks can simply be constructed from two basic units only, namely, the pentagonal and hexagonal pyramids, B_6 and B_7, respectively.
(16) Boustani, I. *Phys. Rev. B* **1997**, *55*, 16426.
(17) Tang, H.; Ismail-Beigi, S. *Phys. Rev. Lett.* **2007**, *99*, 115501.
(18) Zhou, S. M.; Wang, P.; Li, S.; Zhang, B.; Gong, H. C.; Zhang, X. T. *Mater. Lett.* **2009**, *63*, 1680.
(19) Zhu, Y.; Liu, F.; Ding, W.; Guo, X.; Chen, Y. *Angew. Chem.* **2006**, *118*, 7369.
(20) Hohenberg, P.; Kohn, W. *Phys. Rev.* **1964**, *136*, B864.
(21) Kohn, W.; Sham, L. J. *Phys. Rev.* **1965**, *140*, A1133.
(22) Perdew, J. P.; Zunger, A. *Phys. Rev. B* **1981**, *23*, 5048.
(23) Troullier, N.; Martins, J. L. *Phys. Rev. B* **1991**, *43*, 1993.
(24) Kleinman, L.; Bylander, D. M. *Phys. Rev. Lett.* **1982**, *48*, 1425.
(25) Monkhorst, H. J.; Pack, J. D. *Phys. Rev. B* **1976**, *13*, 5188.
(26) Ordejón, P.; Artacho, E.; Soler, J. M. *Phys. Rev. B* **1996**, *53*, R10441.
(27) Soler, J. M.; Artacho, E.; Gale, J. D.; García, A.; Junquera, J.; Ordejón, P.; Sánchez-Portal, D. *J. Phys.: Condens. Matter* **2002**, *14*, 2745.
(28) Quandt, A.; Liu, A. Y.; Boustani, I. *Phys. Rev. B* **2001**, *64*, 125422.
(29) Saito, R.; Dresselhaus, G.; Dresselhaus, M. S. *Physical Properties of Carbon Nanotubes*; Imperial College Press: London, 1998.
(30) Zhao, M.; Zhang, R. Q.; Xia, Y.; Lee, S.-T. *Phys. Rev. B* **2006**, *73*, 195412.
(31) Chernozatonskii, L. A.; Sorokin, P. B.; Fedorov, A. S. *Phys. Solid State* **2006**, *48*, 2021.
(32) Kudin, K. N.; Scuseria, G. E.; Yakobson, B. I. *Phys. Rev. B* **2001**, *64*, 235406.
(33) Seifert, G.; Köhler, Th.; Urbassek, H. M.; Hernández, E.; Frauenheim, Th. *Phys. Rev. B* **2001**, *63*, 193409.
(34) Novoselov, K. S.; Jiang, D.; Schedin, F.; Booth, T. J.; Khotkevich, V. V.; Morozov, S. V.; Geim, A. K. *Proc. Natl. Acad. Sci. U.S.A.* **2005**, *102*, 10451.
(35) Dumitrica, T.; Hua, M.; Yakobson, B. I. *Phys. Rev. B* **2004**, *70*, 241303.
(36) Decker, B. F.; Kasper, J. S. *Acta Crystallogr.* **1959**, *12*, 503.
(37) Hoard, J. L.; Geller, S.; Hughes, R. E. *J. Am. Chem. Soc.* **1951**, *73*, 1892.
(38) Meng, S.; Kaxiras, E.; Zhang, Z. Y. *Nano Lett.* **2007**, *7*, 663.
(39) Tang, H.; Ismail-Bei gi, S. *Phys. Rev. B* **2009**, *80*, 134113.

JP9112014